SCIENCE CHINA
Physics, Mechanics & Astronomy

Network structure of thermonuclear reactions in nuclear landscape

HuanLing Liu, DingDing Han, YuGang Ma and Liang Zhu

Citation: SCIENCE CHINA Physics, Mechanics & Astronomy **63**, 112062 (2020); doi: 10.1007/s11433-020-1552-2

View online: http://engine.scichina.com/doi/10.1007/s11433-020-1552-2

View Table of Contents: http://engine.scichina.com/publisher/scp/journal/SCPMA/63/11

Published by the Science China Press

SCIENCE CHINA
Physics, Mechanics & Astronomy

• Article •
Editor's Focus

November 2020 Vol. 63 No. 11: 112062
https://doi.org/10.1007/s11433-020-1552-2

Editor's Focus

Network structure of thermonuclear reactions in nuclear landscape

HuanLing Liu[1,2,3], DingDing Han[4*], YuGang Ma[1,2*], and Liang Zhu[2,3]

[1] *Key Laboratory of Nuclear Physics and Ion-beam Application (MOE), Institute of Modern Physics, Fudan University, Shanghai 200433, China;*
[2] *Shanghai Institute of Applied Physics, Chinese Academy of Sciences, Shanghai 201800, China;*
[3] *University of the Chinese Academy of Sciences, Beijing 100080, China;*
[4] *School of Information Science and Technology, Fudan University, Shanghai 200433, China*

Received February 7, 2020; accepted March 27, 2020; published online April 28, 2020

Nucleosynthesis is a complex process in astro-nuclear evolution. In this work, we constructed a directed, multi-layer, nuclear reaction network, using the substrate-product method from a thermonuclear reaction database, JINA REACLIB. The network contained four layers, namely *n*-, *p*-, *h*- and *r*-, which correspond to the types of reactions involved in neutrons, protons, ^{4}He and the remaining atomic particles, respectively. The degree values (i.e. numbers of reactions), for three layers of *n*-, *p*-, and *h*-, have a significant correlation with one another, and their topological structures exhibit a similar regularity. However, the *r*-layer has a more complex topological structure compared to the other layers; thus, its correlation of degree values with the other three layers is not as strong as that seen in the other layers. To analyze the motif structure of the nuclear reaction network, we used the software package "mfinder". We identified the most frequent reaction patterns of the interconnections that occurred amongst the different nuclides. This work provides a novel approach to investigating the nuclear reaction network that prevails in the astrophysical context.

nuclear network, motif, topological structure

PACS number(s): 24.10.-i, 24.30.Cz, 25.20.-x, 29.85.-c

Citation: H. L. Liu, D. D. Han, Y. G. Ma, and L. Zhu, Network structure of thermonuclear reactions in nuclear landscape, Sci. China-Phys. Mech. Astron. **63**, 112062 (2020), https://doi.org/10.1007/s11433-020-1552-2

1 Introduction

The nucleosynthesis of light-weight particles into heavier particles associated with the early universe and the corresponding nuclear processes, are of significant interest current nuclear astrophysics investigations [1-15]. Much attention has been given to earlier topics, such as the exploration up to limits of the nuclear landscape and searching for the island of stability [16-23]. The terrestrial nuclear reaction experiments provide a large volume of data for thermonuclear reaction rates. These primarily focus on stable target and based on these many theoretical models have been developed to calculate the binding energy of different nuclides and the cross-sections, plus reaction rates, for different nuclear processes [24-42]. The JINA REACLIB database is a well-known source of thermonuclear reaction rates [43]. The database is continuously updated and snapshotted regularly, by the JINA Collaboration, which aims to compile a complete set of nuclear reaction rates. Importantly, the database contains various kinds of nuclear reactions, critical parameters needed for calculating reaction rates and Q values, etc. This database provides rich resource of information needed for nuclear-related research across various experimental directions.

*Corresponding authors (DingDing Han, email: ddhan@fudan.edu.cn; YuGang Ma, email: mayugang@fudan.edu.cn)

Traditionally, calculations to determine nuclide abundance could be accomplished by solving sets of time-dependent differential equations in the database. However, this approach can be difficult and challenging. In our previous work, we developed an easier alternative method to determine nuclide properties. This method relies on the construction of complex networks to explore the topological characteristics of thermonuclear reactions [44]. The scope of the complex network theory can also extended to social systems and chemical reactions [45-47]. The primary concept was to identify real interacting units as nodes and determine the relationships between the two units as edges. The nodes and edges form the basis of the graphical structure of a network. By using the translation to form networks, the topological characteristics and other hidden features of the real systems can be identified. As an example, self-similar "scale-free" structures with a power-law degree distribution, is present in several systems, such as the Internet network, naturally occurring objects, biological cells and tissues [48-50]. Additional real-world systems that possess a Poisson degree distribution, such as road networks, also exist [51].

Our previous work [44] used the JINA REACLIB database to present a complex network construction for the nuclear reaction that had been previously framed. We utilized the database to explore different nuclei of the network [43]. This complex network is a part of a class of of multi-layer nuclear reaction networks; in which, the constituent four layers namely, n, p, h, and r, are labeled according to each linked edge, with four types of particles, including neutrons, protons, ^{4}He and the remaining atomic particles. It was determined that the nuclear reaction network exhibited a bimodal degree distribution. These findings are very different from those of either the power-law or Poisson distributions. Combining the topological degree values of the nuclei along the stability line, it was determined that over 80% of the stable nuclides follow the same condition $(K^{[r]}_{i,\mathrm{in}} - K^{[r]}_{i,\mathrm{out}} = 2) \bigcap (K_{i,\mathrm{in}} - K_{i,\mathrm{out}} = 0)$, where $K^{[r]}_{i,\mathrm{in}}$, $K^{[r]}_{i,\mathrm{out}}$, $K_{i,\mathrm{in}}$ and $K_{i,\mathrm{out}}$ present the in-coming and out-going degree value of the nuclei in the r-layer and aggregated network, respectively [44]. This novel method can allow for the investigation of a stable nucleus, with a half-life lower than 10^9 years; this is in contrast to traditional methods [52].

Based on our previous success in describing network properties in the nuclear landscapes, here we employ a similar, multi-layer nuclear reaction network, to explore the topological structure and identify the properties of motifs featuring nuclear reaction patterns, for nuclides in different layers. The correlations of degree between the different layers were also investigated. The present work elucidates some novel features of prevailing nuclear reactions in the field of nuclear astrophysics.

2 Multi-layer nuclear reaction networks

There are 8048 nuclides and 82851 nuclear reactions within the JINA nuclear reaction database. The substrate-product method was applied and all nuclei (i.e. nodes) were mapped into a directed un-weighted network, which was labeled by the edge with three special particles (n for neutron, p for proton or h for ^{4}He) as well as r for the remaining particles. For each nucleus (node X), we identified the reactions as either "in-coming" (e.g. $n + Y \rightarrow X$), or "out-going" ($X + n \rightarrow Y$). The number of reactions for each nucleus (node) is represented by the "degree" associated with a particular node. All nuclear reactions can be divided into four classes, based on layer: the n-layer, p-layer, h-layer and r-layer, each "layer" consisted of a specific type of particle involved in a given reaction. Our previous work provides more in-depth information about this process [44]. Using this definition, the degree value of each nucleus, in the landscape, could be calculated within each layer of the nuclear reaction network, as shown in Figure 1. The degree value of each nucleus is plotted on the N-Z plane, with the number of protons Z versus the number of neutrons N. Different degree values are indicated by different colors. These results indicate that the nuclei in the n-layer, p-layer, and h-layer experience a similar degree value distribution on the N-Z plane, while such regular attributes exist in this case, additional values are distributed at the edge of the nuclide map. When the number of protons was greater than 82 (one of magic numbers), the distribution of degree values for the nucleus appears different, which may be attributed to the activity of the neutrons, in the n-, p-, and h-layers. These observations demonstrate that neutrons can also react with the nucleus in the heavy mass region and this leads to some nodes to experience a degree value of 2 in this region; while the p- and h-layers are not impacted. However, the r-layer has a distinctive degree value structure in the N-Z plane. The primary reason for the complexity of the r-layer, is the variety of reactions in which the nuclides can participate in, such as (γ, n), (γ, p), (γ, α), β decay and so on. In order to demonstrate the correlation of degree within each layer, the degree correlation coefficient is defined as:

$$R_{ML} = \frac{\sum_i^N (K_i^M - \bar{K}_i^M)(K_i^L - \bar{K}_i^L)}{\sqrt{\sum_i^N (K_i^M - \bar{K}_i^M)^2}\sqrt{\sum_i^N (K_i^L - \bar{K}_i^L)^2}}, \quad (1)$$

where the K_i^M and K_i^L represent the degree of the ith nucleus in the M layer and L layer, respectively. The $\bar{K}^M$ and $\bar{K}^L$ are the mean degree of all nuclei in the M layer and L layer, respectively. Here the value of N is the number of all nuclides, i.e. 8048, reported in the nuclear chart.

Figures 2 and 3 represent the degree-to-degree correlations and their correlation coefficients, respectively; for every two

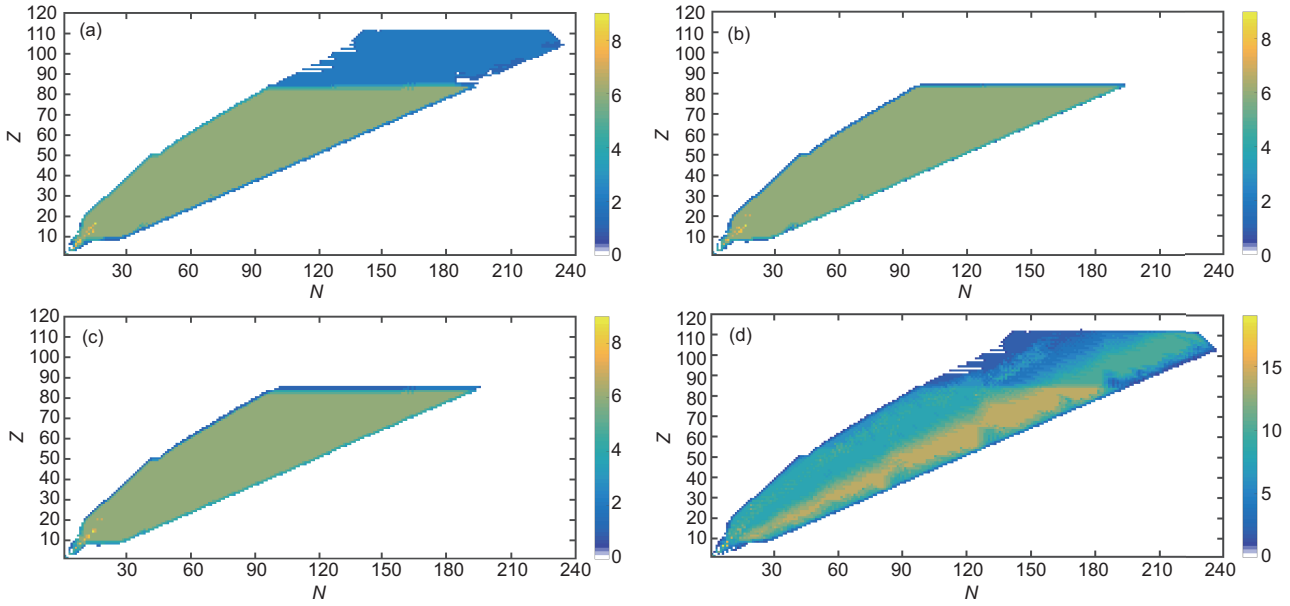

Figure 1 (Color online) The degree value of each nucleus in *n*-layer (a), *p*-layer (b), *h*-layer (c) and *r*-layer (d) plotted in the *N*-*Z* plane. The different colors represent different degree values.

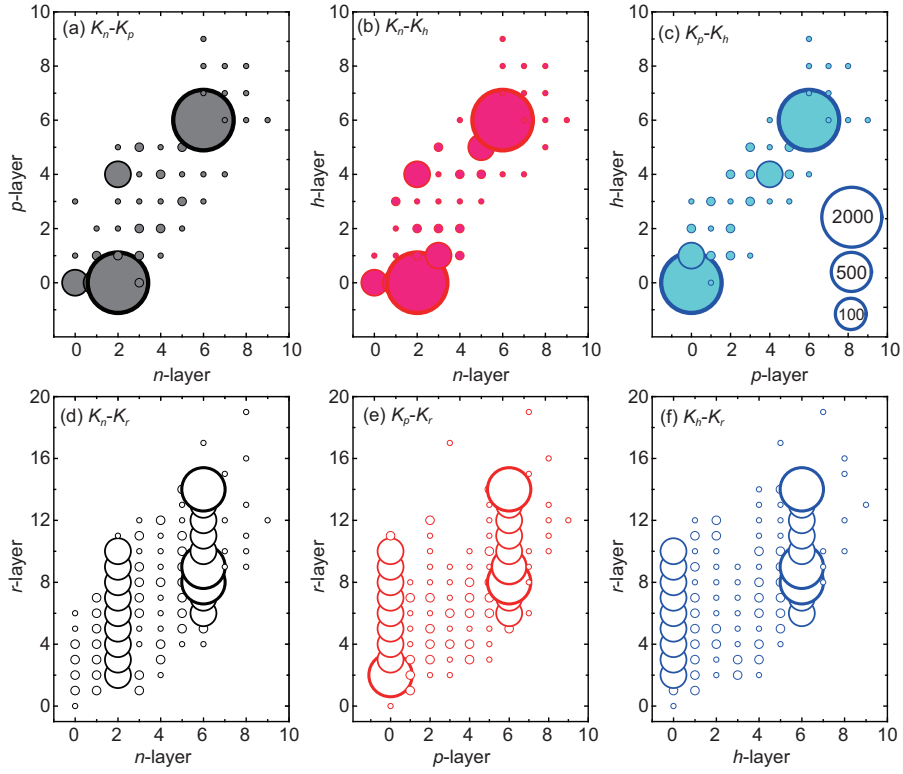

Figure 2 (Color online) Degree-to-degree correlation for each two layers among *n*-, *p*-, *h*- and *r*-layers of the nuclear reaction network. From (a) to (f), figure corresponds to *np*-, *nh*-, *ph*-, *nr*-, *pr*-, and *hr*-layers correlation, respectively. Size of circles in each point represents the frequency of correlation, and its calibration values are inserted.

layers among *n*-, *p*-, *h*- and *r*-layers of the nuclear reaction network. The degree-to-degree correlations of *np*-, *nh*- and *ph*-layers are found to be positive and typically display an almost a linear behavior with a few scatterings. Furthermore, if we see the degree correlation coefficients R_{ML}, i.e. R_{np}, R_{nh}, and R_{ph}, in Figure 3, the values approach one. Of note, the size of the circles within each correlated degree, represents the frequency of the layer-to-layer correlation in Figure 2. The upper panels display the degree distributions of *n*-, *p*-, and *h*-layers, and demonstrated that these are basically bimo-

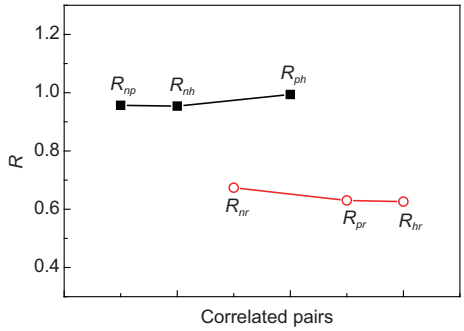

Figure 3 (Color online) Two-layer degree correlation coefficients among *n*-, *p*-, *h*- and *r*-layers of the nuclear reaction network. R_{np}, R_{nh}, R_{ph}, R_{nr}, R_{pr}, and R_{hr} represent correlation of *np*-, *nh*-, *ph*-, *nr*-, *pr*- and *hr*-layers, respectively.

dal, which differ from other typical degree distributions, such as the power-law or Poisson types. The degree-to-degree correlations of the *r*-layer with *n*-, *p*-, and *h*-layers, also display a general positive correlation. However, they seem more diverse in comparison with the correlations among the *n*-, *p*- and *h*-layers. Actually, the degree correlation coefficients of R_{nr}, R_{pr} and R_{hr}, are approximately 0.6. From the degree distributions, shown in Figure 1, the nuclides in the JINA database are similar in structure to those within the *n*-, *p*- and *h*-layers of the reaction networks. However, a relatively complex structure found within the *r*-layer of the reaction network, is observed from the degree-to-degree correlation plots (Figure 2), as well as the correlation coefficients plot R_{ML} (Figure 3).

3 Topological characteristics and motifs

In real systems, repetitive structures can often occur [53,54], such as the regular temporal patterns found in time-varying systems [55,56], or the molecular structures found within organisms [47] and even in the functions or subroutines that occur repeatedly in modern computer programs [57]. Repetitive structures can also be observed in the present reaction system scenario. The degree of each nucleus within the *n*-, *p*- and *h*-layers has a regular value, except at the boundary and light nuclei regions. In network science, these types of topological features are represented as motifs. Even though the numerical and statistical comparisons are made using the degree values and the correlation coefficients of each individual layer, the structure of the motifs require a more detailed description; in which the various possible connections are examined to distinguish the reaction paths are considered in conjunction with the number of linked edges.

The definition of the motifs found within the field of complex network science, is constructed from patterns of the interconnections, occurring in complex networks, at numbers that are significantly greater than those found within randomized networks [53]. In general, the ratio of the number of one motif, found in a real system, to that of a motif found in a random system, which has same size, same number of connected edges and possesses the same degree values of nodes with the real system, is referred to as the score of the motif; represented as: S_i [57], $S_i = (O_i^{(\mathrm{real})} - \langle O_i^{(\mathrm{rand})}\rangle)/\sigma_i^{(\mathrm{rand})}$, where $O_i^{(\mathrm{real})}$ and $\langle O_i^{(\mathrm{rand})}\rangle$ are the occurrence number of the *i*th motif in a real network and the mean occurrence number in a random network, respectively. We assume that $\sigma_i^{(\mathrm{rand})}$ is the variance of the *i*th motif in a random network. Of course, different networks have different motif distributions [57].

The "mfinder" [58], "MAVisto" [59] and the "FANMOD" [60] are the most commonly used statistical software used in motif analysis. In this study, we used the "mfinder" to analyze the structure of the motifs within the nuclear reaction networks, which can equivocate to four or more node motifs in real networks. According to the various combinations found in the origin of the edges within nodes and directions, there are 13 three-node motifs and 199 four-node motifs found within a directed network. Amongst these, five types of three-node motifs and seven types of four-node motifs experience the highest frequencies within the total nuclear reaction networks, shown in Table 1 (where the frequencies of the motifs are provided). Furthermore, it was observed that the number of motifs found within the nuclear reaction network is very large, with frequencies above 10^4. The motif type id238 and id13278 occur at the highest frequencies, when compared to total frequency of occurrence in all three-node and four-node motifs, respectively. The detailed structures of the 13 types of three-node motifs and 7 types of four-node motifs, are shown in Figures 4 and 5, respectively. In Figure 4, motif index id38, id46, id108, id110 and id238 have the greatest statistical significance, shown in Table 1; of which motif id238 is a bidirectional, fully connected, structure. This indicates that most nodes can be transformed into one another within the nuclear reaction networks, such as nucleon absorption and decay. In Figure 5, motif id13278 is

Table 1 Five types of three-node motifs and seven types of four-node motifs which have the highest statistics in the nuclear reaction network

Order	Three-node motifs		Four-node motifs	
	id	Frequency (unit:10^4)	id	Frequency (unit:10^4)
1	38	0.07	922	1.62
2	46	0.66	5064	4.13
3	108	0.71	5068	3.37
4	110	0.59	5086	2.19
5	238	3.87	13150	2.05
6	–	–	13260	4.24
7	–	–	13278	11.27

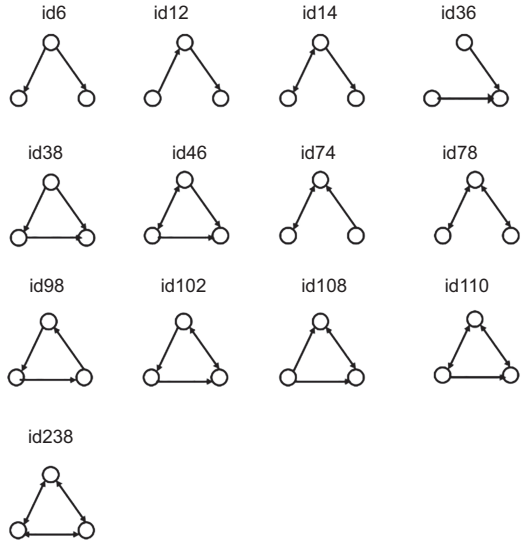

Figure 4 Thirteen types of three-node motifs in the directed network. For a directional single-layer network, we can identify 13 types of three-node motifs, according to various combinations of the directional edges amongst the three nodes. Among them, motifs id38, id46, id108, id110 and id238, occur at the highest statistical significance, of which id238 is observed at the highest frequency. These high statistical motifs indicate that most nodes could be reciprocally transformed and the loop structure is very rich within the nuclear reaction network.

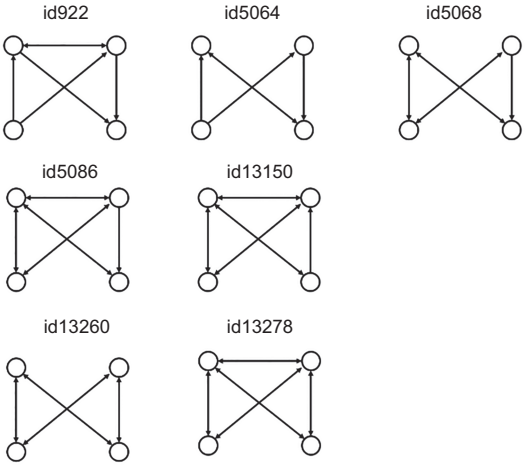

Figure 5 Seven types of four-node motifs experienced the highest statistical significance within the directed network. For a directional, single layer, network, we identified 199 types of four-node motifs according to various combinations of the directional edges amongst the 4 nodes. Here we show that motif id922, id5064, id5068, id5086, id13150, id13260 and id13278, are most frequently occurring four-node motifs. Motif id13278, is a bidirectionally connected structure, except for absence of a pair of nodes and occurs at the highest statistical significance; it can be seen as a superposition of the above mentioned three-node motif id238, as shown in Figure 4.

also a bidirectional and has an almost fully connected structure, except where there is an absence of an edge between node pairs; this motif can be seen as a superposition of the above three-node motif id238. The absence of an edge between a pair of nodes, means that there is no direct reaction pathway between these two nuclei (nodes); therefore, the distance between the two nodes is at least 2 or 3.

4 Discussion

A detailed analysis of a nuclear reaction is difficult using a combination of degree values, for each nucleus within the nuclear landscape in all four layers of the reaction networks, and their traditional motif structures. Additionally, the nodes, such as disseminators, relayers and community cores, often have typical neighboring connection patterns, making it difficult to define the regularity of a structure, based on the same degree of each node [61,62]. Therefore, we proposed a single node motif for the analysis of the characteristics of each nuclear reaction. In this context, by using the proposed method of regarding each nucleus as a motif, the nuclear reaction pathways of each nucleus, within the multi-layer nuclear reaction networks, have been obtained by learning the degree of the in-coming and out-going directions.

From our analysis, we displayed the typical structures of the motifs of the nuclides within the n-, p-, h-layers and the r-layer, shown in Figure 6. In the n-layer, the nucleus located at (N,Z) has in-coming edges from the nuclides located at $(N-1,Z)$, $(N-1,Z+1)$ and $(N+1,Z+2)$, and has out-going edges to the nuclides located at $(N+1,Z)$, $(N+1,Z-1)$ and $(N-1,Z-2)$. These results correspond to the reactions of (n,γ), (n,p) and (n,α), respectively. However, for nuclide with $Z \geq 82$ (i.e. Pb), this kind of n-layer motif vanishes and is replaced by a simpler horizontal structure, i.e. from $(N-1,Z)$ to (N,Z), then to $(N+1,Z)$. In the p-layer, the nucleus located at (N,Z) has in-coming edges from the nuclides located at $(N+2,Z+1)$, $(N+1,Z-1)$ and $(N,Z-1)$, and out-going edges to the nuclides located at $(N-2,Z-1)$, $(N-1,Z+1)$ and $(N,Z+1)$, This corresponds to the reactions of (p,α), (p,n) and (p,γ), respectively. However, as $Z \geq 83$ (i.e. Bi), this type of p-layer motif disappears, and no p-edge as $Z > 84$ is observed. Within the h-layer, the nucleus located at (N,Z) has in-coming edges from the nuclides located at $(N-1,Z-2)$, $(N-2,Z-2)$ and $(N-2,Z-1)$, and out-going edges to the nuclides located at $(N+1,Z+2)$, $(N+2,Z+2)$ and $(N+2,Z+1)$. This corresponds to the reactions of (α,n), (α,γ) and (α,p), respectively. However, as $Z \geq 81$ (i.e. Tl), this type of h-layer motif disappears, therefore, no edges are observed as $Z > 85$. Considering the degree value from the above single-node motif, found within three-layer networks, we discovered that although they have the same degree value, the influences of reactions involving neutron, proton and α-particle, on the change of neutron and proton numbers, differ due to the nuclear reaction law. This results in different topo-

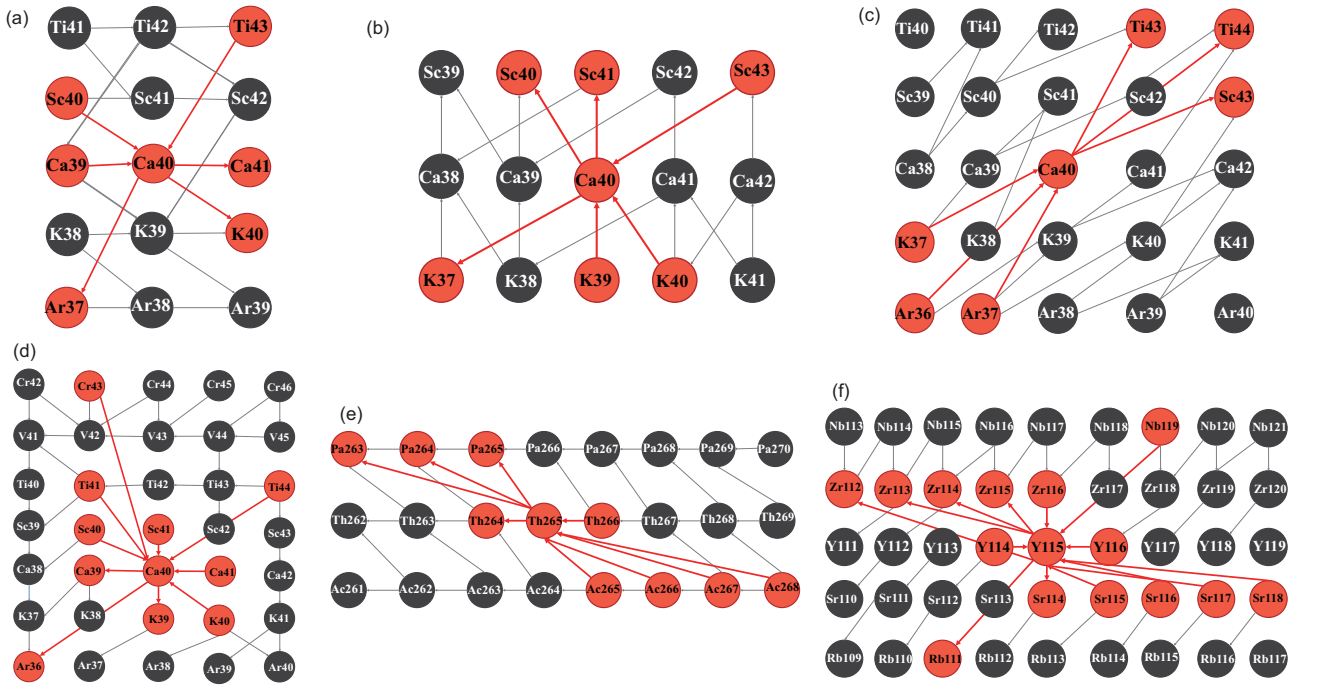

Figure 6 (Color online) Examples of typical topological structures of motifs found in each layer of the nuclear reaction networks. (a)-(c) represent the *n*-, *p*- and *h*-layers, respectively. (d)-(f) represent some typical motifs structures of the *r*-layer. The examples of central nodes are $^{40}_{20}$Ca for (a)-(d), $^{265}_{80}$Th for (e) and $^{115}_{39}$Y (f). Interestingly, even though the value of degrees for *n*-, *p*-, and *h*-layers, the single-node motifs are the same (i.e. $k = 6$). The effects on the change of proton and neutron numbers of the nuclei are different for different layers. This indicates that there is a different topological structure for the *n*-, *p*- and *h*-layer motifs. (d) is a typical *r*-layer motif for proton-rich nuclides, while (e) and (f) represent two major motifs for neutron-rich nuclides. In each plot, the red line illustrating the in-coming or out-going arrow shows the links for the in-coming or out-going edge.

logical structures of the motifs.

For the complex *r*-layer network, the topological structure of the single-node motif is determined by the reactions of the (γ,n), (γ,p), (γ,α), β^+ decay, β^- decay and so on. For the neutron-rich nuclides, typical motifs are shown in Figure 6(e) and (f). For nuclides with $Z \geq 84$ (i.e. Po), their motif structure will transfer the type (f) for lighter nuclides to the type (e) for heavier nuclides. If the proton numbers increase, the motif structure within this region will reduce to a type of motif structure with both in-coming and out-going degrees that are equal to 3. For nuclei located at (N, Z), in-coming edges come from the nuclides located at $(N+1, Z)$, $(N+2, Z-1)$ and $(N+1, Z-1)$, and out-going edges go to the nuclides located at $(N-1, Z)$, $(N-2, Z+1)$ and $(N-1, Z+1)$, respectively. For the proton-rich nuclides, a typical motif structure is shown in Figure 6(d). This is essentially a mirror about $Z = N$ of the motif structure, within the neutron-rich region. This may reflect the reflect the observed symmetrical features found between neutrons and protons. There is additional important information regarding stable nuclides within the *r*-layer motifs. This information can be deduced by comparing the unstable nuclides to the stable nuclides, such as determining the edge difference with a reverse direction. If we take Pb as an example of this comparison, we can see that the direction of the edge, between stable nucleus ^{207}Pb and its neighbor $(N+1, Z-1)$, is opposite to that of the edge between unstable nucleus ^{205}Pb and its neighbor $(N+1, Z-1)$. This noted difference between the stable and unstable nuclides, may explain why the condition of the stable nuclides is the difference of degree in *r*-layer is two, i.e., $K^{[r]}_{i,\text{in}} - K^{[r]}_{i,\text{out}} = 2$. This possible explanation was first proposed in our previous work [44] .

All of the above typical motifs, can be continuously repeated or overlapped within the specific *r*-layer region; or in almost whole *n*-, *p*- and *h*-layers. However, only some nodes within the *r*-layer were observed to have long-range edges. Of importance, we noted that all topological structures revealing motifs, from each layer, in the multi-layer nuclear reaction network, fade away when the proton number becomes greater than the magic number of $Z = 82$, or when the proton number is equal to its neighboring value. This may indicate that the topological structure of the nuclide found in this region become simpler or tend to disappear altogether. This appears to be a global feature for the entire nuclear landscape.

5 Summary

In summary, we constructed a directed, un-weighted, multi-layer nuclear reaction network. This complex network con-

struction consisted of all nuclides and reactions within the JINA REACLIB database. This allowed us to investigate important topological features and motif structures of the nuclear reactions. Importantly, there are four types of edges, namely neutron, proton, ^{4}He and remaining particles; therefore, we present nuclear reaction networks consisting of four-layers, which correspond to the *n*-, *p*-, *h*- and *r*-layers. Using the data from the topological structures of the nuclear reaction networks, we were able to determine that the nuclear reaction networks within the *n*-, *p*- and *h*-layers, experience a regular structure. Therefore, these networks can be categorized as those having repetitive superposition motifs that have spatial features. The *r*-layer network has multiple motifs, but is still categorized as the same for the networks without multiple motifs. All motif structures, regardless of the layer in which they are found, fade away or change shape as the number of protons reaches at or near 82. By comparing the motif structures of typical stable nuclides to those of neighboring, unstable nuclides, in the *r*-layer, we find that the majority of cases only differ is the direction of a certain edge reverse turn, i.e. from the in-coming to the out-going or vice versa. This may also explain why the degree difference, between the in-coming and the out-going, of stable nuclides in the *r*-layer is two [44]. Moreover, it was determined that the degree-to-degree correlations are strong for the *np*-, *nh*-, and *ph*-layers, which typically display near linear behaviors, with the exception of some light scatterings. The degree correlation coefficients, R_{ML}, for the above mention results, approach one. However, the degree-to-degree correlations of the *r*-layer, with *n*-, *p*-, and *h*-layers, are weakly correlated and the degree correlation coefficients were found to be approximately 0.6; this is consistent with different motif structures found within the *n*-, *p*-, *h*-layers from the *r*-layer. This study presents a unique understanding of thermonuclear reactions in astro-nuclear processes. Further studies, that focus on the *r*- and other nuclear reaction processes, involving all the nuclides, may be beneficial.

This work was supported by the National Natural Science Foundation of China (Grant Nos. 11890714, 1421505, 11875133, and 11075057), and the National Key Research and Development Program of China (Grant No. 2018YFB2101302).

1 E. M. Burbidge, G. R. Burbidge, W. A. Fowler, and F. Hoyle, Rev. Mod. Phys. **29**, 547 (1957).
2 H. Schatz, A. Aprahamian, J. Görres, M. Wiescher, T. Rauscher, J. F. Rembges, F. K. Thielemann, B. Pfeiffer, P. Möller, K. L. Kratz, H. Herndl, B. A. Brown, and H. Rebel, Phys. Rep. **294**, 167 (1998).
3 M. Arnould, and S. Goriely, Phys. Rep. **384**, 1 (2003).
4 M. Arnould, S. Goriely, and K. Takahashi, Phys. Rep. **450**, 97 (2007), arXiv: 0705.4512.
5 F. Käppeler, R. Gallino, S. Bisterzo, and W. Aoki, Rev. Mod. Phys. **83**, 157 (2011), arXiv: 1012.5218.
6 J. Chen, D. Keane, Y. G. Ma, A. Tang, and Z. Xu, Phys. Rep. **760**, 1 (2018), arXiv: 1808.09619.
7 A. P. Ji, A. Frebel, A. Chiti, and J. D. Simon, Nature **531**, 610 (2016), arXiv: 1512.01558.
8 H. O. U. Fynbo, et al. (ISOLDE Collaboration), Nature **433**, 136 (2005).
9 Z. D. An, Z. P. Chen, Y. G. Ma, J. K. Yu, Y. Y. Sun, G. T. Fan, Y. J. Li, H. H. Xu, B. S. Huang, and K. Wang, Phys. Rev. C **92**, 045802 (2015), arXiv: 1509.00725.
10 Z. D. An, Y. G. Ma, G. T. Fan, Y. J. Li, Z. P. Chen, and Y. Y. Sun, Astrophys. J. **817**, L5 (2016), arXiv: 1602.01692; Z. D. An, Y. G. Ma, G. T. Fan, Y. J. Li, Z. P. Chen, and Y. Y. Sun, Astrophys. J. **877**, L42 (2019).
11 H. Pais, F. Gulminelli, C. Providncia, and G. Röpke, Nucl. Sci. Tech. **29**, 181 (2018).
12 X. D. Tang, S. B. Ma, X. Fang, B. Bucher, A. Alongi, C. Cahillane, and W. P. Tan, Nucl. Sci. Tech. **30**, 126 (2019).
13 S. B. Ma, L. Y. Zhang, and J. Hu, Nucl. Sci. Tech. **30**, 141 (2019).
14 W. J. Li, Y. G. Ma, G. Q. Zhang, X. G. Deng, M. R. Huang, A. Bonasera, D. Q. Fang, J. Q. Cao, Q. Deng, Y. Q. Wang, and Q. T. Lei, Nucl. Sci. Tech. **30**, 180 (2019).
15 Z. Li, Z. M. Niu, and B. H. Sun, Sci. China-Phys. Mech. Astron. **62**, 982011 (2019).
16 J. Erler, N. Birge, M. Kortelainen, W. Nazarewicz, E. Olsen, A. M. Perhac, and M. Stoitsov, Nature **486**, 509 (2012).
17 R. Wang, and L. W. Chen, Phys. Rev. C **92**, 031303(R) (2015), arXiv: 1410.2498.
18 S. A. Giuliani, Z. Matheson, W. Nazarewicz, E. Olsen, P. G. Reinhard, J. Sadhukhan, B. Schuetrumpf, N. Schunck, and P. Schwerdtfeger, Rev. Mod. Phys. **91**, 011001 (2019).
19 Y. T. Oganessian, F. S. Abdullin, P. D. Bailey, D. E. Benker, M. E. Bennett, S. N. Dmitriev, J. G. Ezold, J. H. Hamilton, R. A. Henderson, M. G. Itkis, Y. V. Lobanov, A. N. Mezentsev, K. J. Moody, S. L. Nelson, A. N. Polyakov, C. E. Porter, A. V. Ramayya, F. D. Riley, J. B. Roberto, M. A. Ryabinin, K. P. Rykaczewski, R. N. Sagaidak, D. A. Shaughnessy, I. V. Shirokovsky, M. A. Stoyer, V. G. Subbotin, R. Sudowe, A. M. Sukhov, Y. S. Tsyganov, V. K. Utyonkov, A. A. Voinov, G. K. Vostokin, and P. A. Wilk, Phys. Rev. Lett. **104**, 142502 (2010).
20 X. B. Yu, L. Zhu, Z. H. Wu, F. Li, J. Su, and C. C. Guo, Nucl. Sci. Tech. **29**, 154 (2018).
21 D. Naderi, and S. A. Alavi, Nucl. Sci. Tech. **29**, 161 (2018).
22 D. Boilley, B. Cauchois, H. Lü, A. Marchix, Y. Abe, and C. Shen, Nucl. Sci. Tech. **29**, 172 (2018).
23 Y. Z. Qian, Sci. China-Phys. Mech. Astron. **61**, 049501 (2018), arXiv: 1801.09554.
24 H. Herndl, and B. A. Brown, Nucl. Phys. A **627**, 35 (1997).
25 S. Ota, G. Christian, G. Lotay, W. N. Catford, E. A. Bennett, S. Dede, D. T. Doherty, S. Hallam, J. Hooker, C. Hunt, H. Jayatissa, A. Matta, M. Moukaddam, G. V. Rogachev, A. Saastamoinen, J. A. Tostevin, S. Upadhyayula, and R. Wilkinson, Phys. Lett. B **802**, 135256 (2020), arXiv: 2001.08206.
26 P. Liu, J. Chen, D. Keane, Z. Xu, and Y. G. Ma, Chin. Phys. C **43**, 124001 (2019), arXiv: 1908.03134.
27 S. Zhang, J. C. Wang, A. Bonasera, M. R. Huang, H. Zheng, G. Q. Zhang, Z. Kohley, Y. G. Ma, and S. J. Yennello, Chin. Phys. C **43**, 064102 (2019), arXiv: 1903.09772.
28 Y. T. Wang, D. Q. Fang, K. Wang, X. X. Xu, L. J. Sun, P. F. Bao, Z. Bai, X. G. Cao, Z. T. Dai, B. Ding, W. B. He, M. R. Huang, S. L. Jin, C. J. Lin, M. Lv, L. X. Liu, Y. Li, P. Ma, J. B. Ma, J. S. Wang, S. T. Wang, J. G. Wang, H. W. Wang, S. Q. Ye, Y. Y. Yang, C. L. Zhou, M. H. Zhao, H. Q. Zhang, Y. G. Ma, and W. Q. Shen, Phys. Lett. B **784**, 12 (2018).
29 Y. T. Wang, D. Q. Fang, K. Wang, X. X. Xu, L. J. Sun, Z. Bai, P. F. Bao, X. G. Cao, Z. T. Dai, B. Ding, W. B. He, M. R. Huang, S. L. Jin, Y. Li, C. J. Lin, L. X. Liu, M. Lv, J. B. Ma, P. Ma, H. W. Wang, J. G.

Wang, J. S. Wang, S. T. Wang, Y. Y. Yang, S. Q. Ye, H. Q. Zhang, M. H. Zhao, C. L. Zhou, Y. G. Ma, and W. Q. Shen, Eur. Phys. J. A **54**, 107 (2018).
30 K. Wang, D. Q. Fang, Y. T. Wang, X. X. Xu, L. J. Sun, Z. Bai, M. R. Huang, S. L. Jin, C. Li, H. Li, J. Li, X. F. Li, C. J. Lin, J. B. Ma, P. Ma, W. H. Ma, M. W. Nie, C. Z. Shi, H. W. Wang, J. G. Wang, J. S. Wang, L. Yang, Y. Y. Yang, H. Q. Zhang, Y. J. Zhou, Y. G. Ma, and W. Q. Shen, Int. J. Mod. Phys. E **27**, 1850014 (2018).
31 X. X. Xu, C. J. Lin, L. J. Sun, J. S. Wang, Y. H. Lam, J. Lee, D. Q. Fang, Z. H. Li, N. A. Smirnova, C. X. Yuan, L. Yang, Y. T. Wang, J. Li, N. R. Ma, K. Wang, H. L. Zang, H. W. Wang, C. Li, M. L. Liu, J. G. Wang, C. Z. Shi, M. W. Nie, X. F. Li, H. Li, J. B. Ma, P. Ma, S. L. Jin, M. R. Huang, Z. Bai, F. Yang, H. M. Jia, Z. H. Liu, D. X. Wang, Y. Y. Yang, Y. J. Zhou, W. H. Ma, J. Chen, Z. G. Hu, M. Wang, Y. H. Zhang, X. W. Ma, X. H. Zhou, Y. G. Ma, H. S. Xu, G. Q. Xiao, and H. Q. Zhang, Phys. Lett. B **766**, 312 (2017).
32 Y. G. Ma, D. Q. Fang, X. Y. Sun, P. Zhou, Y. Togano, N. Aoi, H. Baba, X. Z. Cai, X. G. Cao, J. G. Chen, Y. Fu, W. Guo, Y. Hara, T. Honda, Z. G. Hu, K. Ieki, Y. Ishibashi, Y. Ito, N. Iwasa, S. Kanno, T. Kawabata, H. Kimura, Y. Kondo, K. Kurita, M. Kurokawa, T. Moriguchi, H. Murakami, H. Ooishi, K. Okada, S. Ota, A. Ozawa, H. Sakurai, S. Shimoura, R. Shioda, E. Takeshita, S. Takeuchi, W. D. Tian, H. W. Wang, J. S. Wang, M. Wang, K. Yamada, Y. Yamada, Y. Yasuda, K. Yoneda, G. Q. Zhang, and T. Motobayashi, Phys. Lett. B **743**, 306 (2015), arXiv: 1503.05631.
33 Z. H. Li, Y. J. Li, J. Su, S. Q. Yan, Y. B. Wang, B. Guo, D. Nan, E. T. Li, L. Gan, and W. P. Liu, Sci. China-Phys. Mech. Astron. **62**, 032021 (2019).
34 W. Jiang, Y. L. Ye, Z. H. Li, C. J. Lin, Q. T. Li, Y. C. Ge, J. L. Lou, D. X. Jiang, J. Li, Z. Y. Tian, J. Feng, B. Yang, Z. H. Yang, J. Chen, H. L. Zang, Q. Liu, P. J. Li, Z. Q. Chen, Y. Zhang, Y. Liu, X. H. Sun, J. Ma, H. M. Jia, X. X. Xu, L. Yang, N. R. Ma, and L. J. Sun, Sci. China-Phys. Mech. Astron. **60**, 062011 (2017).
35 X. Y. Yun, D. Y. Pang, Y. P. Xu, Z. Zhang, R. R. Xu, Z. Y. Ma, and C. X. Yuan, Sci. China-Phys. Mech. Astron. **63**, 222011 (2020).
36 W. Liu, J. L. Lou, Y. L. Ye, and D. Y. Pang, Nucl. Sci. Tech. **31**, 20 (2020).
37 D. Wu, C. L. Bai, H. Sagawa, Z. Q. Song, and H. Q. Zhang, Nucl. Sci. Tech. **31**, 14 (2020).
38 D. Benzaid, S. Bentridi, A. Kerraci, and N. Amrani, Nucl. Sci. Tech. **31**, 9 (2020).
39 H. R. Guo, Y. L. Han, and C. H. Cai, Nucl. Sci. Tech. **30**, 13 (2019).
40 Y. Liu, and Y. L. Ye, Nucl. Sci. Tech. **29**, 184 (2018).
41 R. Baldık, and A. Yılmaz, Nucl. Sci. Tech. **29**, 156 (2018).
42 C. Yalçın, Nucl. Sci. Tech. **28**, 113 (2017).
43 R. H. Cyburt, A. M. Amthor, R. Ferguson, Z. Meisel, K. Smith, S. Warren, A. Heger, R. D. Hoffman, T. Rauscher, A. Sakharuk, H. Schatz, F. K. Thielemann, and M. Wiescher, Astrophys. J. Suppl. Ser. **189**, 240 (2010).
44 L. Zhu, Y. G. Ma, Q. Chen, and D. D. Han, Sci. Rep. **6**, 31882 (2016), arXiv: 1608.07812.
45 D. J. Watts, and S. H. Strogatz, Nature **393**, 440 (1998).
46 C. C. Jolley, and T. Douglas, Astrophys. J. **722**, 1921 (2010).
47 C. Jolley, and T. Douglas, Astrobiology **12**, 29 (2012).
48 A. L. Barabási, and R. Albert, Science **286**, 509 (1999), arXiv: cond-mat/9910332.
49 S. Boccaletti, V. Latora, Y. Moreno, M. Chavez, and D. Hwang, Phys. Rep. **424**, 175 (2006).
50 L. F. Costa, O. N. Oliveira Jr., G. Travieso, F. A. Rodrigues, P. R. Villas Boas, L. Antiqueira, M. P. Viana, and L. E. Correa Rocha, Adv. Phys. **60**, 329 (2011), arXiv: 0711.3199.
51 A. L. Barabási, *Network Science* (Cambridge University Press, Cambridge, 2016).
52 M. Thoennessen, Rep. Prog. Phys. **67**, 1187 (2004).
53 R. Milo, S. Shen-Orr, S. Itzkovitz, N. Kashtan, D. Chklovskii, and U. Alon, Science **298**, 824 (2002).
54 N. H. Tran, K. P. Choi, and L. Zhang, Nat. Commun. **4**, 2241 (2013).
55 L. Kovanen, K. Kaski, J. Kertesz, and J. Saramaki, Proc. Natl. Acad. Sci. **110**, 18070 (2013), arXiv: 1302.2563.
56 L. Kovanen, M. Karsai, K. Kaski, J. Kertész, and J. Saramäki, J. Stat. Mech. **2011**, P11005 (2011), arXiv: 1107.5646.
57 U. Alon, Nat. Rev. Genet. **8**, 450 (2007).
58 N. Kashtan, S. Itzkovitz, R. Milo, and U. Alon, *Mfinder Tool Guide*, Technical Report (Weizmann Institute of Science, Rehovot, 2002).
59 F. Schreiber, and H. Schwobbermeyer, Bioinformatics **21**, 3572 (2005).
60 S. Wernicke, and F. Rasche, Bioinformatics **22**, 1152 (2006).
61 L. F. Costa, and F. A. Rodrigues, Europhys. Lett. **85**, 48001 (2009).
62 L. F. Costa, F. A. Rodrigues, C. C. Hilgetag, and M. Kaiser, Europhys. Lett. **87**, 18008 (2009), arXiv: 1003.3084.